





## BRIEF COMMUNICATION

# Appositional long bone growth: Implications for measuring cross-sectional geometry

Helen K. Kurki<sup>1</sup>  | Sydney Holland<sup>1,2</sup> | Marla MacKinnon<sup>1</sup> | Libby Cowgill<sup>3</sup>  | Benjamin Osipov<sup>4</sup>  | Lesley Harrington<sup>5</sup> 

<sup>1</sup>Department of Anthropology, University of Victoria, Victoria, British Columbia, Canada

<sup>2</sup>Department of Anthropology, Western University, London, Ontario, Canada

<sup>3</sup>Department of Anthropology, University of Missouri, Columbia, Missouri, USA

<sup>4</sup>Department of Orthopaedic Surgery, University of California, Davis Health, Sacramento, California, USA

<sup>5</sup>Department of Anthropology, University of Alberta, Edmonton, Alberta, Canada

## Correspondence

Helen K. Kurki, Department of Anthropology, University of Victoria, Victoria, British Columbia, Canada.

Email: [hkurki@uvic.ca](mailto:hkurki@uvic.ca)

## Funding information

Natural Sciences and Engineering Research Council of Canada, Grant/Award Number: RGPGP-2014-00054

## Abstract

**Objectives:** As growth at the periosteal and endosteal surfaces varies with age, cross-sectional geometric (CSG) properties derived from periosteal (“solid”) contours may not produce comparable results to those from endosteal and periosteal contours (“true”), contrary to findings from adults. Error in CSG properties derived from the “solid” sections is compared with “true” sections in a sample of archeologically derived skeletons with estimated dental ages ranging from 1.5 months to 23.5 years.

**Materials and Methods:** Cross sections were extracted from 3D surface models, and endosteal contours were located from biplanar radiographs for 56 femora and 59 humeri. Polar second moment of area ( $J$ ), cross-sectional shape ( $I_{\max}/I_{\min}$ ), and polar section modulus ( $Z_p$ ) were calculated from solid and true sections. Relationships between solid and true properties were examined with least squares regression. Multiple regression examined the effect of age and % cortical area on solid section CSG error.

**Results:** While correlations were high ( $R^2 = 0.72\text{--}0.99$ , all  $p < 0.001$ ), the results indicate that solid CSG properties are not within an acceptable error range (%SEE of  $\leq 8.0$ , and %PE of  $\leq 5.0$ ) of true CSG. Error was most affected by %CA, while estimated age was not correlated with %CA, %PE, or percent difference of true-solid CSG.

**Discussion:** Periosteal contours alone should not be used to calculate CSG properties from individuals during the period of growth and development. Variation in bone growth and/or adaptive responses independent of age may account for the inconsistent age effects.

## KEYWORDS

biomechanics, bone growth, cross-sectional geometry, femur, humerus

## 1 | INTRODUCTION

Long bone cross-sectional geometric properties (i.e., diaphyseal robusticity) have become a key means to examine habitual activity in archeological populations, addressing questions about changes to mobility, division of labor, unimanual versus bimanual activities (e.g., asymmetry), and other activity related patterns through time and space

(e.g., Cameron & Pfeiffer, 2014; Macintosh et al., 2017; Miller et al., 2018; Ruff et al., 2015; Shaw & Stock, 2013; Sparacello et al., 2011; Stock et al., 2013; see also Ruff, 2019 for review). Throughout life, bone modeling and remodeling deposit and replace bone tissue around the diaphysis in response to the direction and magnitude of habitual loading, through a process known as bone functional adaptation (Lanyon et al., 1982; Lanyon & Rubin, 1984;

Ruff, 2019; Ruff et al., 2006; Ruff & Hayes, 1983), resulting in changes to bone size and shape. Measuring the distribution of bone tissue in cross-section can therefore tell us about how the bone was loaded by body mass and muscle action over the life course. Bony response to loading is greatest during growth and development and reduced in adulthood, after bone growth is completed, though remodeling continues (Pearson & Lieberman, 2004; Ruff et al., 1994; Ruff et al., 2006).

The examination of adult diaphyseal robusticity has long dominated studies while immature remains have attracted less attention, perhaps due to sample size issues, the potential for variation in growth timing and physiological status to affect cortical bone distribution, or a lack of attention to children in the archeological record. Despite these challenges, an increasing recognition that children are active members of their communities, with important social and economic roles, has started to shift attention towards archaeologies of childhood and adolescence (e.g., Baxter, 2005; Lewis, 2016; Nowell, 2021). Further, given the central role of the growth and development period for establishing adult skeletal characteristics, investigating the habitual activity patterns of immature individuals can be particularly informative (Pearson & Lieberman, 2004). Several recent studies (e.g., Cowgill, 2010, 2014; Harrington & Osipov, 2018; Mizushima et al., 2016; Osipov et al., 2016; Osipov et al., 2020) have examined diaphyseal robusticity in immature remains from archeological and paleoanthropological contexts to understand patterns of activity in these populations before adulthood. The study of activity patterns during growth can tell us much about group mobility, when children started engaging in adult habitual activities, as well as underlying factors affecting variation in bone adaptive responses. Examination of immature diaphyseal robusticity is, therefore, interesting in its own right.

Physiological stress during the growth and development period can influence the rate and pattern of bone deposition and resorption on the periosteal and endosteal surfaces, altering cortical thickness (Garn, Guzman, & Wagner, 1969; Ruff, Walker, & Larsen, 1994). Thus, cortical thickness is one measure used to examine stress responses during growth in archeological samples (Gooderham et al., 2019; Mays et al., 2009; Temple et al., 2014), but may also impact diaphyseal cross-sectional properties. In light of the interactions among factors (e.g., dietary, mechanical) influencing cortical bone thickness and distribution, Ruff (2019) has demonstrated that a bone with a thin cortex is actually stronger, relative to one with a thicker cortex, if the bone tissue is distributed farther from the neutral axis or centroid. For bending loads, it is the tissue furthest from the neutral axis of the bone, and for torsion, that from the centroid, that is most subject to mechanical stress (Jepsen, 2009), therefore it is the location and shape of the outer (periosteal) contour that most captures loading history (Macintosh et al., 2013; Ruff, 2019). Sparacello and Pearson (2010) demonstrate this mathematically in their detailed discussion of the calculation of bending rigidities ( $I_x$ , second moment of area of  $x$  axis). Temple et al. (2014) came to similar conclusions about the ability of diaphyses to adapt to high mechanical loading in the face of reductions in bone formation due to malnutrition, while Lazenby (1990) demonstrates that endosteal resorption due to aging requires

only a small amount of compensatory periosteal bone apposition to maintain bone function. Further, Eleazer and Jankauskas (2016) demonstrate that bone strength is maintained in individuals with skeletal evidence of chronic metabolic stress. Their findings are consistent with Ruff's hypotheses since endosteal bone loss was accompanied by increased periosteal bone deposition in these chronically stressed individuals.

Various methods of measuring cross-sectional geometric properties have been employed and tested. Ideally, one has a direct image of the endosteal and periosteal contours from a computed tomography (CT) scan or a fortuitous break in the long bone. While CT scanning is becoming more accessible to researchers, factors such as cost, curatorial policies, or descendant community stipulations can limit the opportunity to image skeletal material using CT. Stock (2002) also noted that image resolution in CT scans could influence the reliability of this method. A common alternative to CT scanning is to create cross section images by replicating the periosteal contour using either a ring of casting material (silicone or latex) placed around the diaphysis or a slice from a 3D surface model of the bone, and locating the corresponding endosteal surface using measurements taken from biplanar radiographs (in anteroposterior and mediolateral views) (O'Neill & Ruff, 2004; Ruff, 2019; Sylvester et al., 2010; Trinkaus & Ruff, 1989). Identifying the location of the endosteal contour in this way enables reconstruction of the medullary cavity, which may not be concentric with the periosteal cross-section (Sparacello & Pearson, 2010). X-ray also requires exposing the skeleton to radiation, which like CT scanning, can be limited by cost, access, or curatorial or descendant community decisions. Several studies have suggested that cross-sectional properties can be accurately estimated from periosteal contours only, such as those derived from 3D surface scans of the bone (Davies et al., 2012; Sparacello & Pearson, 2010; Stock & Shaw, 2007). Whole bone scans also allow for the rapid generation of cross sections from multiple locations along the diaphysis, enabling a more complex examination of shape and robusticity variation within bones (e.g., Davies & Stock, 2014; Shaw et al., 2014). The robusticity estimates using periosteal contours have been shown to fall within generally acceptable error ranges, at least for cross sections near the midshaft (Davies et al., 2012; Macintosh et al., 2013; Sparacello & Pearson, 2010; Stock & Shaw, 2007). An important caveat here is that these methods are considered acceptable (that is, the estimation error is within acceptable limits) for population level comparisons, not for estimation of CSG properties for individuals (Ruff & Larsen, 2014; Sparacello & Pearson, 2010). Macintosh et al. (2013) demonstrated that percentage cortical area (%CA) has the strongest impact on error associated with this method and therefore regions towards the proximal or distal ends of the bone produce higher error. Sparacello and Pearson (2010) examined the effects of %CA on comparisons of population mean CSG properties generated using periosteal contours only and found limited impact of %CA or differences in %CA among populations on these types of analyses. These studies only examined cross-sectional properties from skeletons of adults, but they note that because of the role %CA plays in estimation error from a periosteal-only method, and the variability in activity at the endosteal surface during both growth

and development (deposition and resorption) and aging (resorption) of bone, these methods may not be reliable for juvenile age groups (Macintosh et al., 2013; Sparacello & Pearson, 2010). The effectiveness of the periosteal-only method has not been tested on immature skeletal material.

The current study examines whether cross-sectional geometric properties in an ontogenetic sample derived from only the periosteal contour produce acceptable results when compared with properties including both the periosteal and endosteal contours. Following Macintosh et al. (2013), this study examines the cross-sectional properties  $J$ , the polar second moment of area (a measure of bone torsional rigidity),  $Z_p$ , the polar section modulus (a measure of torsional and twice average bending strength), and  $I_{max}/I_{min}$ , the ratio of the maximum and minimum second moment areas (perpendicular maximum and minimum bending rigidities) as an index of diaphyseal shape. The  $I_{max}/I_{min}$  ratio provides an indication of the degree of circularity versus ellipticity of the diaphyseal cross section. Long bones loaded in a dominant direction will have a more elliptical shape, whereas bones loaded equally in a variety of directions will be more circular. More mobile population tend to have more elliptical lower limb bone diaphyses since walking loads the diaphyses predominantly in an antero-posterior direction (Pearson et al., 2014; Ruff, 1994; Stock & Pfeiffer, 2001, 2004). Examination of measurement error in cross-sectional properties derived from the periosteal surface only relative to those measured from endosteal and periosteal contours, allows for an assessment of the importance of including the endosteal contour when considering biomechanical properties in juveniles. As any solid section (periosteal contour only) will over-estimate cross-sectional parameters by virtue of containing more bone tissue than a section with the medullary cavity (periosteal and endosteal contours), it is not expected that the values from both methods will be equal. However, the question is whether a consistent developmental trajectory of cross-sectional parameters is found within a sample using both methods. If so, then periosteal-only methods could be used for comparisons among ontogenetic samples. If not, then variation within and across the developmental period in the rate and pattern of periosteal bone deposition and endosteal bone resorption may mean that periosteal-only methods are not reliable for such samples.

## 2 | MATERIALS AND METHODS

### 2.1 | Skeletal sample

Fifty-six femora and 59 humeri from a total of 62 individuals were used for this study. The estimated age at death of these individuals ranges between 1.5 months to 23.5 years. As this sample includes young adults whose skeletal growth is complete, the sample represents an ontogenetic sample that includes the “endpoint” of growth. Some individuals had both a femur and humerus present, but preservation issues meant that both elements could not be analyzed from all individuals. All of the individuals included in the study were from foraging populations and thus considered to be highly active. In total, 21 individuals were from

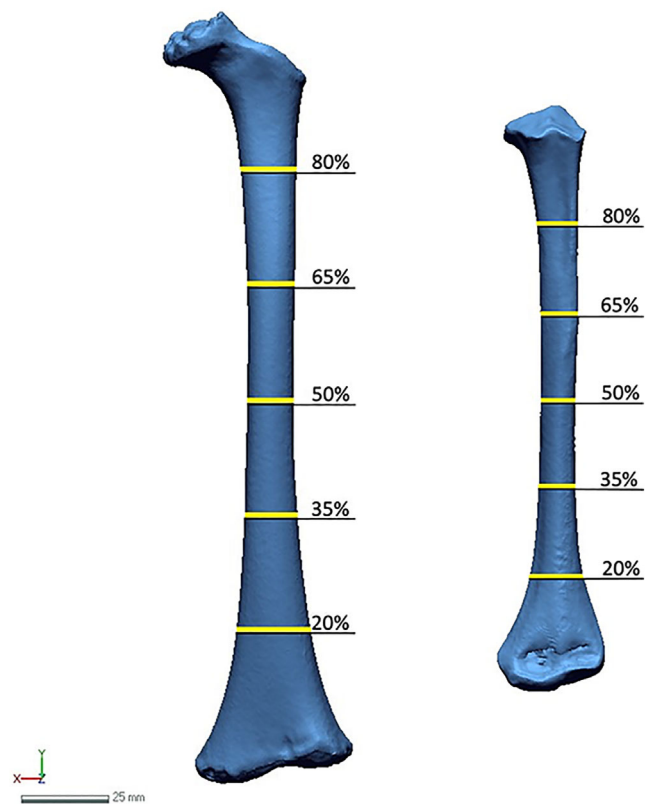


**FIGURE 1** Digital 3D models of a femur (left) and a humerus (right) showing the locations (as % length) at which cross sections were extracted

the Later Stone Age southern Africa (age mean [years] = 7.97,  $SD = 5.37$ ), and 41 were Sadlermiut from Native Point, Nunavut (age mean [years] = 7.41,  $SD = 7.30$ ). The LSA sample represents terrestrial foragers from savanna, fynbos, and karoo ecosystems, and have dates ranging from  $1860 \pm 50$  to  $220 \pm 50$  (BP) (Morris, 1992; Pfeiffer & Harrington, 2011). These skeletons are curated at the Albany Museum in Grahamstown, South Africa and the McGregor Museum in Kimberley, South Africa. The Sadlermiut population lived in the Canadian Arctic for at least 500 years prior to the winter of 1902–03 when they succumbed to an introduced disease (Merbs, 1983). A group of Sadlermiut individuals from the site of Native Point on Southampton Island have been radiocarbon dated to a range of 1308–1890 CE (Coltrain et al., 2004). These skeletons are curated on behalf of the Inuit Heritage Trust at the Canadian Museum of History in Ottawa, Canada. Ages at death of the individuals were estimated using the QMUL Atlas of Tooth Development and Eruption (AlQahtani et al., 2010). For skeletons missing dental material, age at death was estimated using sample-specific regression equations of femur length and/or ilium breadth on dental age (Cardoso et al., 2014; Cardoso et al., 2017; Cowgill, 2010).

### 2.2 | Cross-sectional geometry

Three-dimensional digital surface scans were collected using a Konica Virtuoso structured light scanner or a NextEngine surface laser

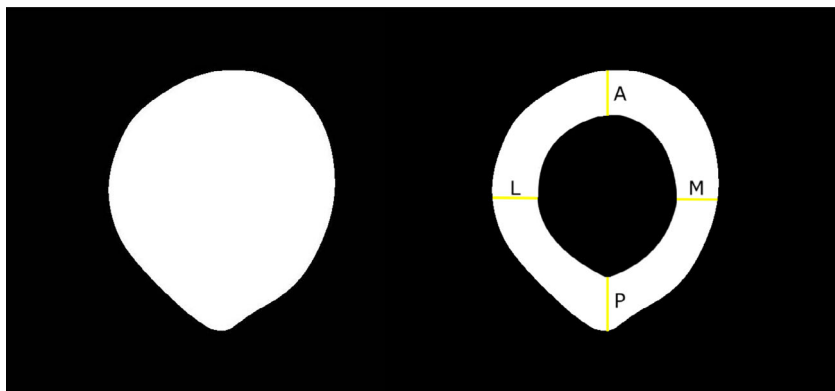


**FIGURE 2** Examples of solid (left) and true (right) cross-sectional images. Locations of the anterior, posterior, medial, and lateral cortical measurements used to estimate the endosteal contour are indicated on the cross-sectional image on the right

**TABLE 1** Descriptive statistics for percent difference (%DIF) for humerus and femur by diaphyseal location

Location (%) <sup>a</sup>	Femur				Humerus			
	<i>n</i>	Mean (%)	<i>SD</i>	Range	<i>n</i>	Mean (%)	<i>SD</i>	Range
<i>J</i>								
20	53	-50.8	8.9	-68.3, -29.5	49	-34.2	15.3	-63.6, -4.8
35	53	-25.9	9.3	-44.4, -5.3	52	-18.6	10.4	-48.8, -2.4
50	53	-13.5	7.9	-32.2, -2.4	58	-16.4	9.2	-38.7, -2.9
65	54	-15.2	8.1	-37.5, -5.0	54	-21.4	10.4	-45.8, -4.2
80	37	-37.0	14.3	-61.9, -6.7	44	-35.6	14.7	-63.1, -9.5
<i>Z<sub>p</sub></i>								
20	53	-51.4	9.1	-69.0, -28.2	49	-34.3	15.6	-64.3, -4.3
35	53	-27.3	9.5	-47.9, -6.2	52	-19.1	10.8	-49.4, -2.5
50	53	-13.4	8.1	-33.2, -1.3	58	-16.7	9.2	-39.8, -1.4
65	54	-16.0	8.4	-39.6, -3.0	54	-22.3	10.9	-49.2, -3.8
80	37	-37.8	14.9	-65.9, -7.0	44	-35.4	15.4	-64.0, -9.1
<i>I<sub>max</sub>/I<sub>min</sub></i>								
20	53	-13.3	7.0	-26.8, 9.1	49	-6.7	6.7	-23.0, 4.8
35	53	-2.8	4.4	-19.4, 13.3	52	-1.4	2.7	-8.7, 7.8
50	53	-0.8	2.8	-8.1, 12.3	58	-3.3	3.6	-12.6, 3.6
65	54	-1.4	3.7	-10.0, 9.7	54	-3.1	4.2	-13.5, 7.4
80	37	-2.1	6.6	-20.0, 13.2	44	-4.9	4.4	-22.8, 7.2

<sup>a</sup>Location of cross-section as % of bone length. Zero % is the distal end of the long bone.

scanner, which were then fused into 3D models using GeoMagic Design X (3D Systems) or ScanStudio (NextEngine Inc.). Cross sections were extracted from the 3D models at 20%, 35%, 50%, 65%, and 80% locations along the length of the bone (Figure 1) in Design X. Given the variation in maturational stages of the femur and humerus across the age range of the study sample, bone length was measured as unfused diaphyseal length in individuals without fused epiphyses, or as total bone length for individuals with one or more fused epiphyses as diaphysis-only lengths could not be determined on the 3D bone models for these individuals. This method of identifying locations on the diaphysis as a percentage of length differs from other approaches (e.g., Ruff, 2002, 2003a, 2003b). Diaphyseal cross-sectional images were generated for both the

periosteal contour only (solid) and the periosteal plus endosteal contours (true) (Figure 2). To create the true images, cortical thicknesses of the anterior, posterior, medial, and lateral positions were measured from biplanar radiographs at each diaphyseal location, and the endosteal contour was drawn following the periosteal contour (i.e., not as an ellipse) in ImageJ software (Fiji package; Schindelin et al., 2012; Figure 2). These images are, therefore, still approximations of a true cross-section, but since they include the position of the medullary cavity they more accurately represent the actual bone distribution in the cross-section than do the solid sections. Cross-sectional geometric properties from both solid and true cross section images were calculated using the *BoneJ* plugin for ImageJ (Doube et al., 2010).

## 2.3 | Statistical analyses

All statistical analyses were completed using R Version 3.6.1 (R Core Team, 2019), and examples of the code are provided in the Supplementary Materials. The cross-sectional geometric properties  $J$  (polar second moment of area),  $I_{\max}/I_{\min}$  (ratio of second moments of area), and  $Z_p$  (polar section modulus) were analyzed at each section location. The data were transformed using the natural logarithm to correct for violations of regression assumptions when utilizing the raw data. Differences between the true and solid CSG parameters at each location were investigated in two ways. First, the percentage differences (%DIF) between the two values (Equation 1) were calculated.

$$\%DIF = \left( \frac{\text{true} - \text{solid}}{\text{solid}} \right) \times 100 \quad (1)$$

Second, following Macintosh et al. (2013) ordinary least squares regression of true parameters onto solid parameters was applied, and error was quantified using three values: (1) percent standard error of the estimate (%SEE) for natural log-transformed data following Ruff (2003c) (Equation 2), (2) absolute percent prediction error (%PE) (Equation 3), and (3) directional percent prediction error (Bias %PE) (Equation 4).

$$\%SEE = \exp(\text{SEE} + 4.6052) - 100 \quad (2)$$

$$\%PE = \frac{|\text{observed} - \text{estimated}|}{\text{estimated}} \times 100\% \quad (3)$$

$$\text{Bias}\%PE = \frac{\text{observed} - \text{estimated}}{\text{estimated}} \times 100\% \quad (4)$$

Percent prediction errors (%PE and Bias %PE) for the true CSG values were calculated using the measured values ("observed") and the back-transformed predicted CSG values ("estimated"). Back-transformed values were not corrected for de-transformation bias since the amount of bias was determined to be small (<2%). To be consistent with previous studies, %SEE of  $\leq 8.0$ , and %PE of  $\leq 5.0$  were considered acceptable error rates (Davies et al., 2012; Macintosh et al., 2013; O'Neill & Ruff, 2004; Sparacello & Pearson, 2010; Stock, 2002; Stock & Shaw, 2007). The %DIF provides a measure of error that is independent of the regression analysis given the affects age variation may have on these relationships. Multiple linear regression analyses were performed for both  $J$  and  $Z_p$  to test the effects of percent cortical area (%CA = (cortical area/total area)  $\times$  100%),  $I_{\max}/I_{\min}$ , and age on the estimation of true parameters from those derived using only the periosteal contour. The relationships of age with %DIF, %CA, %PE, and Bias %PE were examined through correlation analyses.

**TABLE 2** Results of linear regression of true cross-sectional geometry (CSG) on solid CSG properties

Location <sup>a</sup>	Femur					Humerus				
	R <sup>2</sup>	b <sub>0</sub>	b <sub>1</sub>	95% CI <sup>¶</sup>	p-Value <sup>§</sup>	R <sup>2</sup>	b <sub>0</sub>	b <sub>1</sub>	95% CI <sup>¶</sup>	p-Value <sup>§</sup>
<i>J</i> solid vs. <i>J</i> true										
80	0.976	-1.52	1.11	1.05-1.17	<0.001	0.950	-0.96	1.06	0.99-1.14	<0.001
65	0.996	-0.01	0.98	0.96-1.00	<0.001	0.988	-0.33	1.01	0.98-1.04	<0.001
50	0.998	0.11	0.97	0.95-0.98	<0.001	0.994	-0.01	0.97	0.95-1.00	<0.001
35	0.993	-0.10	0.98	0.95-1.00	<0.001	0.991	0.07	0.96	0.93-0.98	<0.001
20	0.982	-0.84	1.01	0.97-1.05	<0.001	0.958	-0.83	1.05	0.99-1.12	<0.001
<i>Z<sub>p</sub></i> solid vs. <i>Z<sub>p</sub></i> true										
80	0.957	-1.68	1.17	1.09-1.26	<0.001	0.913	-0.96	1.08	0.98-1.19	<0.001
65	0.992	-0.04	0.98	0.95-1.00	<0.001	0.977	-0.40	1.02	0.98-1.07	<0.001
50	0.995	0.09	0.96	0.94-0.98	<0.001	0.988	-0.09	0.98	0.95-1.01	<0.001
35	0.986	-0.17	0.98	0.94-1.01	<0.001	0.980	0.03	0.95	0.91-0.99	<0.001
20	0.968	-0.86	1.02	0.96-1.07	<0.001	0.921	-0.84	1.07	0.98-1.16	<0.001
<i>I<sub>max</sub>/I<sub>min</sub></i> solid vs. <i>I<sub>max</sub>/I<sub>min</sub></i> true										
80	0.711	-0.03	1.02	0.79-1.24	<0.001	0.923	0.00	0.90	0.82-0.98	<0.001
65	0.946	0.02	0.89	0.83-0.95	<0.001	0.933	0.02	0.89	0.82-0.96	<0.001
50	0.957	-0.01	0.99	0.93-1.05	<0.001	0.953	0.00	0.91	0.86-0.96	<0.001
35	0.875	0.00	0.88	0.78-0.97	<0.001	0.938	0.00	0.92	0.85-0.99	<0.001
20	0.897	0.03	0.72	0.65-0.78	<0.001	0.795	-0.01	0.90	0.76-1.03	<0.001

Notes: b<sub>0</sub>, regression constant; b<sub>1</sub>, regression coefficient.

<sup>a</sup>Location of cross-section as % of bone length. Zero % is the distal end of the long bone.

<sup>§</sup>p-Value of model.

<sup>¶</sup>95% confidence interval for the regression coefficient (slope); if the CI does not include 1.0 then the relationship is non-isometric at  $p < 0.05$ ; CI <1.0 indicates negative allometry, CI >1.0 indicates positive allometry.

### 3 | RESULTS

#### 3.1 | Percentage differences

The percent differences (%DIF) between the true and solid CSG parameters ( $J$ ,  $Z_p$ , and  $I_{\max}/I_{\min}$ ) are summarized in Table 1. Patterns are generally similar for both the humerus and femur, and all %DIFs are negative values, as expected. For all three parameters, mean %DIF is lowest at midshaft and increases at locations toward the ends of the long bone, as does the variability in %DIF—in general—as illustrated by the standard deviation and range values. Mean %DIFs are quite large for  $J$  and  $Z_p$ , ranging from  $-13.4\%$  to  $-51.4\%$ . The 20% location of the femur shows a substantial increase for both parameters ( $J$  mean =  $-50.8\%$ ,  $Z_p$  mean =  $-51.4\%$ ) relative to the other locations.

#### 3.2 | Bivariate regression and error

The results of the bivariate linear regression and error analyses are provided in Tables 2 and 3, respectively. For both the humerus and femur, all three CSG parameters ( $J$ ,  $Z_p$ ,  $I_{\max}/I_{\min}$ ) show similar results. The relationships between the true and solid values are strongest near the midshaft (50% location,  $R^2$  range = 0.953–0.998), and weaker

toward the ends of the diaphysis (20% and 80% locations,  $R^2$  range = 0.711–0.976). These relationships are also predominantly isometric (95% confidence interval of the slope includes 1.0), except for  $I_{\max}/I_{\min}$  where negative allometry is more prevalent. Despite the strength of these relationships, the error rates are only within acceptable limits for  $I_{\max}/I_{\min}$  except for the 20% location of the humerus (% SEE = 7.54; %PE = 5.85). No diaphyseal locations produce acceptable error rates for  $J$  and  $Z_p$ . Error rates increase with distance from the midshaft (50%), and are slightly greater for the humerus relative to the femur. Average directional prediction errors (Bias %PE) are variable for both bones (range = 0.03–3.11), though the trend for all parameters is for error to be lowest and slightly positive toward the midshaft, with higher positive bias toward the diaphyseal ends (i.e., models underestimate the true CSG parameter). However, while mean error is near zero, the large standard deviations indicate substantial variation in individual error values and no consistent patterns of over- or underestimation of true values.

#### 3.3 | Multiple regression

The results of the multiple linear regression analyses are provided in Table 4. At all locations on both bones, the solid CSG parameter and %CA are significant predictors for true  $J$  and  $Z_p$  values

**TABLE 3** Error statistics for prediction of true CSG property from solid CSG property

Location <sup>a</sup>	Femur					Humerus				
	%SEE <sup>b</sup>	%PE		Bias %PE		%SEE <sup>b</sup>	%PE		Bias %PE	
		Mean	SD	Mean	SD		Mean	SD	Mean	SD
<i>J</i> solid vs. <i>J</i> true										
80	22.35	17.25	9.77	1.92	19.94	28.21	19.68	12.89	2.84	23.54
65	10.23	7.28	5.60	0.44	9.23	15.04	10.89	7.47	0.91	13.26
50	8.28	5.84	4.85	0.30	7.63	11.75	8.57	6.13	0.58	10.58
35	13.11	9.89	6.88	0.72	12.10	13.32	9.04	7.25	0.72	11.64
20	20.67	14.46	11.34	1.67	18.41	26.74	19.69	11.68	2.63	22.92
<i>Z<sub>p</sub></i> solid vs. <i>Z<sub>p</sub></i> true										
80	23.87	17.92	10.28	2.13	20.76	29.71	20.75	13.17	3.11	24.58
65	10.81	7.95	5.59	0.49	9.77	15.97	11.42	8.13	1.02	14.07
50	8.83	6.31	5.08	0.34	8.14	12.15	8.86	6.29	0.62	10.91
35	13.99	10.81	6.95	0.82	12.91	14.54	10.20	7.36	0.85	12.63
20	21.39	14.83	11.82	1.78	18.99	27.65	19.88	12.47	2.78	23.47
<i>I<sub>max</sub>/I<sub>min</sub></i> solid vs. <i>I<sub>max</sub>/I<sub>min</sub></i> true										
80	7.32	4.98	4.55	0.23	6.79	4.70	2.88	3.23	0.10	4.35
65	3.49	2.48	2.34	0.06	3.43	4.07	3.16	2.28	0.08	3.92
50	2.79	1.82	2.08	0.04	2.77	3.51	2.61	2.12	0.06	3.38
35	4.47	2.97	3.10	0.09	4.31	2.59	1.76	1.82	0.03	2.54
20	5.31	3.90	3.36	0.11	5.13	7.54	5.85	3.92	0.25	7.08

<sup>a</sup>Location of cross-section as % of bone length. Zero % is the distal end of the long bone.

<sup>b</sup>%SEE from the linear regression of true CSG property on solid CSG property (see Table 2).



**TABLE 4** Multiple regression results of true CSG properties on solid CSG properties, estimated age, percent cortical area, and diaphyseal shape

Location <sup>a</sup>	Variable	Femur				Humerus			
		<i>J</i>		<i>Z<sub>p</sub></i>		<i>J</i>		<i>Z<sub>p</sub></i>	
		<i>R</i> <sup>2</sup>	<i>p</i> -Value	<i>R</i> <sup>2</sup>	<i>p</i> -Value	<i>R</i> <sup>2</sup>	<i>p</i> -Value	<i>R</i> <sup>2</sup>	<i>p</i> -Value
80	Solid	0.998	<0.001	0.994	<0.001	0.997	<0.001	0.995	<0.001
	Age	-	0.162	-	0.109	-	0.252	-	0.209
	%CA <sup>b</sup>	-	<0.001	-	<0.001	-	<0.001	-	<0.001
	<i>I<sub>max</sub>/I<sub>min</sub></i>	-	0.084	-	0.187	-	0.029	-	0.006
65	Solid	>0.999	<0.001	0.999	<0.001	0.999	<0.001	0.998	<0.001
	Age	-	0.302	-	0.997	-	0.985	-	0.170
	%CA	-	<0.001	-	<0.001	-	<0.001	-	<0.001
	<i>I<sub>max</sub>/I<sub>min</sub></i>	-	0.294	-	0.960	-	0.644	-	0.066
50	Solid	>0.999	<0.001	>0.999	<0.001	>0.999	<0.001	0.999	<0.001
	Age	-	0.012	-	0.418	-	0.065	-	0.364
	%CA	-	<0.001	-	<0.001	-	<0.001	-	<0.001
	<i>I<sub>max</sub>/I<sub>min</sub></i>	-	0.465	-	0.055	-	0.053	-	0.033
35	Solid	>0.999	<0.001	0.999	<0.001	0.999	<0.001	0.998	<0.001
	Age	-	0.065	-	0.244	-	0.345	-	0.420
	%CA	-	<0.001	-	<0.001	-	<0.001	-	<0.001
	<i>I<sub>max</sub>/I<sub>min</sub></i>	-	0.491	-	0.093	-	0.134	-	0.009
20	Solid	0.999	<0.001	0.998	<0.001	0.997	<0.001	0.992	<0.001
	Age	-	0.020	-	0.120	-	0.512	-	0.453
	%CA	-	<0.001	-	<0.001	-	<0.001	-	<0.001
	<i>I<sub>max</sub>/I<sub>min</sub></i>	-	0.795	-	0.532	-	0.530	-	0.378

Notes: *p*-Values < 0.05 are italicized.

<sup>a</sup>Location of cross-section as % of bone length. Zero % is distal end of long bone.

<sup>b</sup>Percent cortical area.

( $p < 0.001$ ). At the 35%, 50%, and 80% locations on the humerus, true  $I_{max}/I_{min}$  is a significant predictor of  $Z_p$  ( $p \leq 0.05$ ), but only at the humerus 80% location ( $p = 0.029$ ) for  $J$ . True  $I_{max}/I_{min}$  is not a significant predictor at any location of the femur for either parameter. Age is also not a significant predictor of true CSG parameters, with the exception of  $J$  at the 50% and 20% locations of the femur ( $p = 0.012$ , 0.020, respectively); however, multicollinearity assessments indicate substantial relationships between age and the CSG parameters (see Table S1). Further, if more a conservative alpha value is adopted due to the multiple tests undertaken (e.g.,  $\alpha = 0.001$  or even  $\alpha = 0.01$ ), neither age nor  $I_{max}/I_{min}$  remain significant predictors for any model.

### 3.4 | Correlations with estimated age-at-death

Relationships between estimated age, and %CA, %DIF, and prediction error (%PE and Bias %PE) were investigated through correlation analyses. Overall, age does not appear to be consistently correlated with %CA across bone locations for either the humerus or femur (Table 5,

**TABLE 5** Results of correlation analysis of estimated age and percent cortical area

Location <sup>a</sup>	<i>r</i>	95% CI	<i>p</i> -Value
Femur			
80	0.58	0.31, 0.76	0.000
65	-0.18	-0.43, 0.09	0.196
50	-0.47	-0.66, -0.23	0.000
35	-0.25	-0.48, 0.02	0.075
20	0.03	-0.24, 0.30	0.826
Humerus			
80	0.32	-0.03, 0.56	0.032
65	0.21	-0.06, 0.45	0.124
50	-0.16	-0.40, 0.10	0.229
35	-0.28	-0.52, 0.01	0.041
20	0.46	0.21, 0.66	0.001

Notes: *p*-Values < 0.05 are italicized.

<sup>a</sup>Location of cross-section as % of bone length. Zero % is the distal end of the long bone.

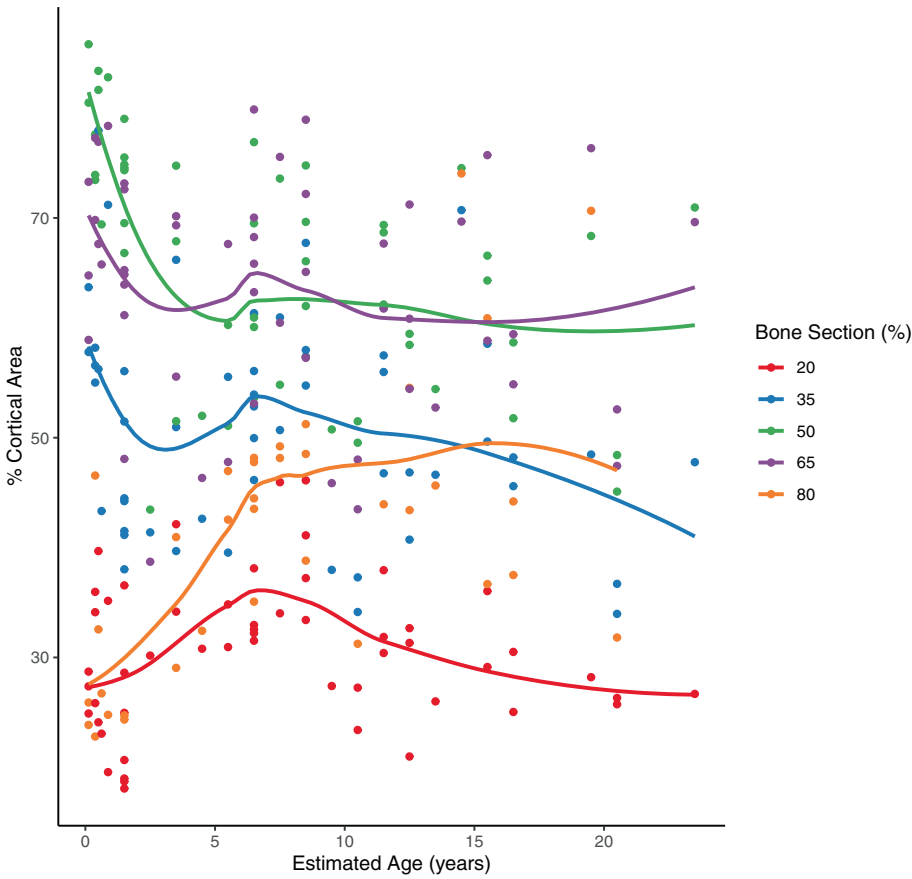


**FIGURE 3** Bivariate plot of percent cortical area (%CA) and estimated age at death (years) at five diaphyseal locations of the femur

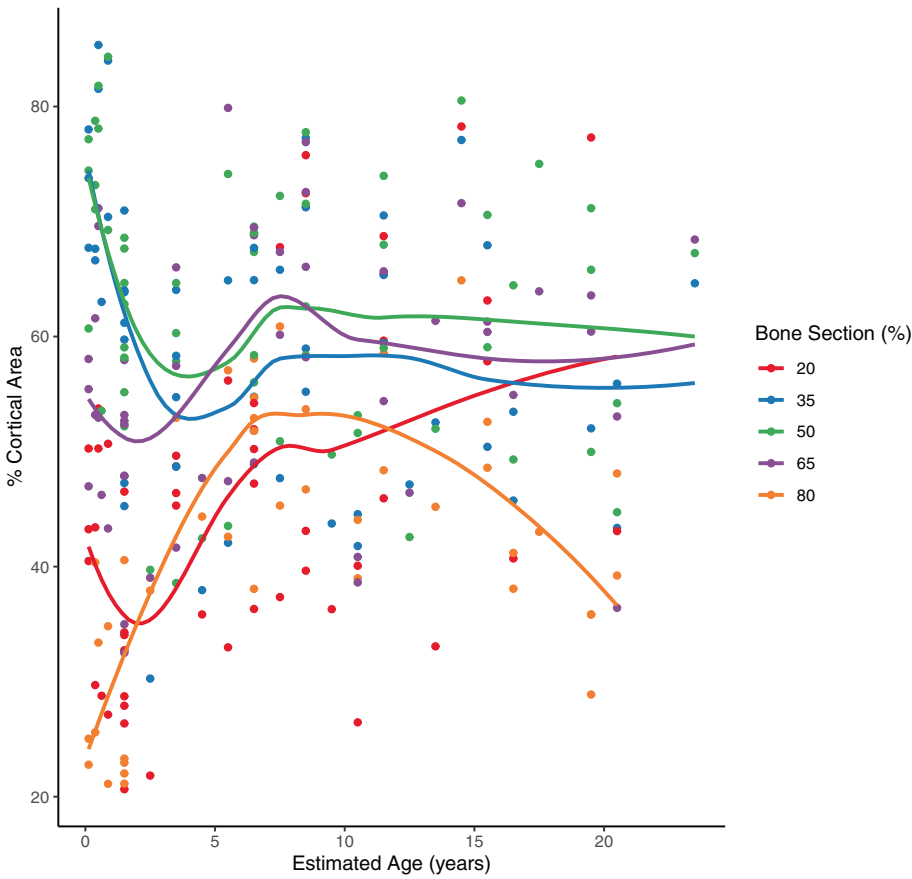


**FIGURE 4** Bivariate plot of percent cortical area (%CA) and estimated age at death (years) at five diaphyseal locations of the humerus



**TABLE 6** Results of correlation analysis of estimated age and percent error

Location <sup>a</sup>	%DIF			%PE			Bias %PE		
	<i>r</i>	95% CI	<i>p</i> -Value	<i>r</i>	95% CI	<i>p</i> -Value	<i>r</i>	95% CI	<i>p</i> -Value
<i>J</i>									
Femur									
80	0.58	0.32, 0.76	<0.001	0.14	-0.19, 0.45	0.390	0.15	-0.18, 0.45	0.382
65	-0.15	-0.40, 0.12	0.264	0.13	-0.14, 0.38	0.348	0.13	-0.14, 0.38	0.353
50	-0.43	-0.63, -0.18	0.001	0.34	0.08, 0.56	0.013	0.10	-0.18, 0.36	0.496
35	-0.23	-0.47, 0.04	0.102	0.01	-0.26, 0.28	0.963	0.03	-0.24, 0.30	0.838
20	0.10	-0.17, 0.36	0.465	-0.20	-0.44, 0.08	0.161	0.03	-0.24, 0.30	0.846
Humerus									
80	0.37	0.08, 0.60	0.013	-0.26	-0.52, -0.03	0.080	0.15	-0.15, 0.43	0.329
65	0.22	-0.05, 0.46	0.112	-0.02	-0.25, 0.29	0.884	0.12	-0.15, 0.38	0.370
50	-0.13	-0.38, 0.13	0.324	0.16	-0.11, 0.40	0.201	0.16	-0.11, 0.40	0.242
35	-0.22	-0.47, 0.05	0.052	0.09	-0.19, 0.35	0.533	0.17	-0.11, 0.42	0.240
20	0.45	0.20, 0.65	0.001	0.14	-0.15, 0.40	0.340	0.27	-0.01, 0.51	0.061
<i>Z<sub>p</sub></i>									
Femur									
80	0.58	0.31, 0.76	<0.001	0.13	-0.20, 0.44	0.438	0.13	-0.21, 0.46	0.460
65	-0.12	-0.37, 0.16	0.404	0.10	-0.16, 0.36	0.442	0.11	-0.16, 0.37	0.424
50	-0.36	-0.057, -0.10	0.008	0.33	0.07, 0.55	0.015	0.12	-0.15, 0.38	0.389
35	-0.16	-0.41, 0.12	0.257	0.08	-0.20, 0.34	0.573	0.03	-0.24, 0.29	0.849
20	0.09	-0.18, 0.35	0.525	-0.20	-0.45, 0.07	0.142	0.01	-0.26, 0.28	0.962
Humerus									
80	0.39	0.10, 0.61	0.009	-0.34	-0.58, -0.05	0.023	0.17	-0.13, 0.45	0.261
65	0.27	0.00, 0.50	0.049	-0.01	-0.14, 0.38	0.353	0.13	-0.14, 0.38	0.353
50	-0.01	-0.26, 0.25	0.969	0.04	-0.21, 0.30	0.752	0.16	-0.10, 0.40	0.227
35	-0.15	-0.41, 0.12	0.276	0.08	-0.20, 0.34	0.590	0.17	-0.11, 0.42	0.233
20	0.46	0.21, 0.66	0.001	0.17	-0.11, 0.43	0.239	0.28	-0.00, 0.52	0.050
<i>I<sub>max</sub>/I<sub>min</sub></i>									
Femur									
80	0.39	0.08, 0.64	0.016	-0.22	-0.51, 0.11	0.183	0.39	0.07, 0.63	0.018
65	0.12	-0.15, 0.38	0.372	0.37	0.11, 0.58	0.006	0.14	-0.13, 0.39	0.315
50	0.11	-0.16, 0.37	0.431	0.42	0.18, 0.62	0.001	0.11	-0.17, 0.37	0.437
35	0.50	0.26, 0.68	<0.001	0.07	-0.20, 0.33	0.617	0.30	0.03, 0.52	0.031
20	0.55	0.34, 0.72	<0.001	-0.15	-0.40, 0.12	0.280	0.27	0.00, 0.50	0.050
Humerus									
80	0.03	-0.27, 0.32	0.846	-0.24	-0.50, 0.06	0.117	-0.11	-0.40, 0.19	0.467
65	-0.13	-0.39, 0.14	0.339	-0.27	-0.50, -0.01	0.046	-0.10	-0.35, 0.18	0.493
50	-0.19	-0.43, 0.07	0.144	-0.12	-0.37, 0.14	0.350	0.01	-0.25, 0.27	0.929
35	-0.01	-0.28, 0.26	0.936	-0.08	-0.34, 0.20	0.581	0.05	-0.22, 0.32	0.718
20	0.20	-0.09, 0.45	0.170	0.11	-0.18, 0.38	0.447	0.20	-0.08, 0.46	0.165

Notes: *p*-Values < 0.05 are italicized.

<sup>a</sup>Location of cross-section as % of bone length. Zero % is the distal end of the long bone.

Figures 3 and 4; Figures S1 and S2 break these down by sub-sample). For the humerus, the 80%, 35% and 20% locations show low to moderate correlations, and in opposite directions (80% *r* = 0.32,

*p* = 0.032; 35%: *r* = -0.28, *p* = 0.041; 20%: *r* = 0.46, *p* = 0.001), and for the femur only the 80% and 50% locations show moderate correlations, again in opposite directions (80%: *r* = 0.58, *p* < 0.001; 50%

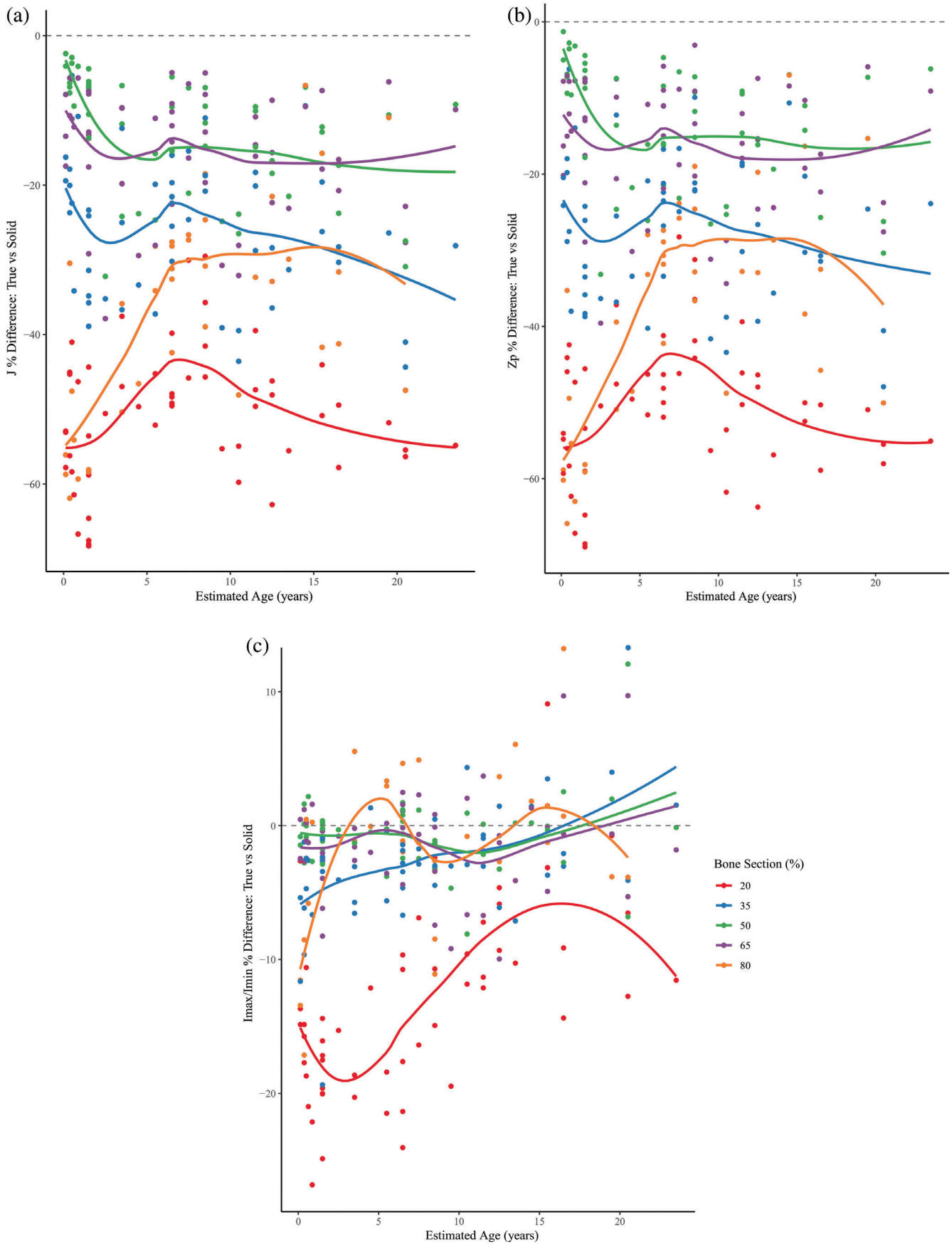


**FIGURE 5** Bivariate plot of percent difference: True - solid CSG (%DIF) and estimated age at death (years) at five diaphyseal locations of the femur. CSG parameters are a) *J*, b) *Z<sub>p</sub>*, and c) *I<sub>max</sub>/I<sub>min</sub>*

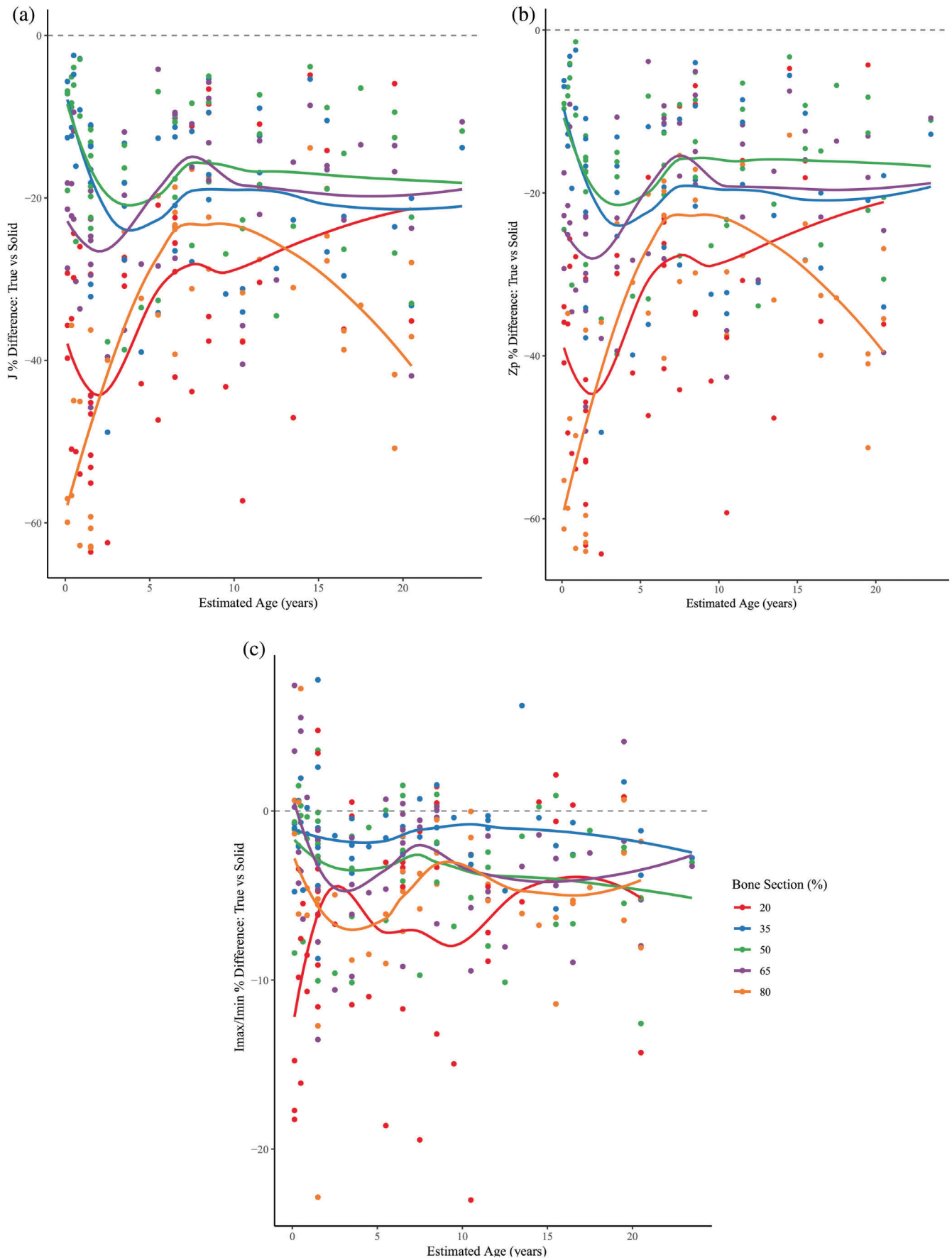


**FIGURE 6** Bivariate plot of percent difference: True - solid CSG (%DIF) and estimated age at death (years) at five diaphyseal locations of the humerus. CSG parameters are a)  $J$ , b)  $Z_p$ , and c)  $I_{max}/I_{min}$

Location <sup>a</sup>	Current study ontogenetic sample				Adults (Macintosh et al., 2013)	
	<i>n</i>	Mean (%)	Range (%)	CV <sup>b</sup>	Mean (%)	Range (%)
<i>Femur</i>						
80	37	41.4	22.8–74.0	30.0	52.4	43.3–67.7
65	54	63.1	38.7–79.9	16.2	79.6	59.2–85.1
50	53	65.5	43.5–85.8	16.6	80.7	68.8–87.1
35	53	51.0	34.0–78.0	19.6	68.8	57.3–77.4
20	53	30.3	18.1–46.1	21.8	47.8	36.6–57.5
<i>Humerus</i>						
80	44	45.0	21.1–71.3	32.7	49.2	40.7–59.9
65	54	59.6	32.5–79.9	21.0	64.3	54.5–76.2
50	58	62.6	38.6–84.3	18.3	69.4	59.9–77.4
35	52	56.3	30.3–85.3	19.9	72.8	64.0–84.5
20	49	42.5	20.6–78.3	30.0	75.3	60.8–87.3

<sup>a</sup>Location of cross-section as % of bone length. Zero % is the distal end of the long bone.

<sup>b</sup>Coefficient of variation = (standard deviation/mean) × 100.

$r = -0.45$ ,  $p < 0.001$ ). Table 6 provides the correlation results for % DIF, %PE, and Bias %PE with age. For all three error measures, where present, correlations are low to moderate in strength and often occur in opposite directions, increasing and decreasing error at different locations on the bone. For example, for %DIF the 80% location of the femur shows significant positive correlations with age for both  $J$  and  $Z_p$ , whereas the 50% location shows negative correlations. Diaphyseal shape ( $I_{max}/I_{min}$ ) only displays significant correlations of %DIF with age for the distal femur (35% and 20% locations), while the humerus shows no correlations. The patterns of correlations for %PE and Bias %PE are more erratic across CSG parameters and diaphyseal locations. With a more conservative alpha value (e.g.,  $\alpha = 0.001$  or even  $\alpha = 0.01$ ), few of these relationships remain statistically significant supporting the overall conclusion that estimated age is generally not correlated with %CA or error. When broken down by sub-sample (Later Stone Age and Sadlermiut) there are differences between the groups in %CA by age which likely produce the differences in error, but what underlies the sub-sample differences is %CA – the effect of %CA on error remains consistent in both groups (see Section 4 and Supplemental Materials).

Figures 5 and 6 illustrate %DIF across age in the sample (Figures S3 and S4 provide sample specific relationships). For  $J$  and  $Z_p$  the 50% and 65% locations of the femur, and 35% and 50% locations of the humerus show similar patterns—a rapid increase in the %DIF across infancy, followed by a leveling off at around 6–7 years of age. The 65% location of the humerus appears to catch up to the 35% and 50% locations around this time as well. The remaining locations are much more variable across age and with larger %DIF values.  $I_{max}/I_{min}$  shows lower %DIF and more consistency across age for the 35%, 50% and 65% locations of both bones. There is also high variability in %DIF for a given age, as evidenced by the broad scatter of data points in these figures (see also %DIF SD and range in Table 1). Plots of %PE and Bias %PE with age are provided in Figures S5–S12.

**TABLE 7** Descriptive statistics for percent cortical area for ontogenetic study sample and adults from Macintosh et al. (2013)

## 4 | DISCUSSION

This study investigated whether the use of solid cross-sections (including only the periosteal contour) would produce CSG values within an acceptable error range of true values (calculated including the periosteal and endosteal contours) for immature femora and humeri. Given the results, the use of periosteal-only contours (solid cross-section) for estimation for CSG properties in immature skeletal samples cannot be recommended. For  $J$  and  $Z_p$ , no diaphyseal location produced error rates within acceptable limits. Error was slightly higher at all locations for the humerus than for the femur, though the differences tended to be minor. The diaphyseal shape index ( $I_{max}/I_{min}$ ) did produce error rates in the acceptable range for almost all locations for both bones. There was also little directional bias in the %PE for most measures, suggesting no consistent pattern of under- or overestimation of a CSG value in the solid cross-sections. The lower error for the shape index is not surprising since it is a ratio of two parameters, the maximum and minimum second moments of area, respectively, and we might expect the effect of ignoring the endosteal contour for the calculation of the solid cross-section values would be similar for both  $I_{max}$  and  $I_{min}$ , keeping the ratio between them similar compared with the ratio of the true values (Ruff & Larsen, 2014; Stock & Shaw, 2007). However, given the high error seen in the solid CSG values for  $J$  and  $Z_p$ , the values of  $I_{max}$  and  $I_{min}$  themselves would likely also contain substantial error, rendering them unreliable on their own. Unless the only goal of an analysis was to compare diaphyseal shapes, there appears to be little justification for using solid cross-sections for immature samples.

In addition to error measured in relation to the linear regression model of true and solid cross-section CSG parameters, error was also measured as the percent difference between true and solid values (% DIF). This measure too showed high error for  $J$  and  $Z_p$ , but lower for diaphyseal shape. As the relationship between %DIF and age appears to stabilize for  $J$  and  $Z_p$  at around age 6–7 years (Figures 5 and 6), it

may be questioned whether solid cross-sections could be a valid alternative for immature samples from mid-childhood and older. To test this, true CSG was regressed on solid CSG using a reduced sample of individuals of 6.5 years and older (Tables S3 and S4). However, while %SEE and %PE did decrease somewhat across the CSG parameters and locations, the only parameters that fall within the acceptable limits remain  $I_{\max}/I_{\min}$  for all locations except 80% on both bones.

Sparacello and Pearson (2010) and Macintosh et al. (2013) both found that %CA had the most impact on differences between true and solid CSG values. That is, lower %CA results in higher error. For the ontogenetic sample in the current study this was also the case, as %CA had the largest effect, after true CSG, in the multiple regression analyses. The fact that age produced inconsistent results in these regressions, and accounts for only a small amount of the model variation where it is significant suggests that any age-related effects are largely mediated through variation in %CA. As well, for all three CSG parameters, error rates are lowest near midshaft (e.g., 50%), and higher towards the proximal/distal ends (e.g., 80% and 20%). Cortical thickness, and therefore %CA, is greater near the midshaft than towards the ends of the diaphysis (Table 7), which may account for this pattern in the error rates along the bone. Further, variation in %CA (e.g., coefficient of variation) is also higher at locations further from midshaft, where error is greater. Work in progress will further investigate the patterns of %CA with age.

Table 7 compares %CA mean, ranges, and CVs from the current study with those for the adults of Macintosh et al.'s (2013) sample. Maximum %CA in the ontogenetic sample is similar or even greater than that seen in the adults, however the mean and minimum %CA are substantially lower in our sample at all locations. Percent cortical area does not increase consistently with age in the ontogenetic sample, therefore the difference in %CA mean and range compared with the adult sample is not accounted for by age-related increases in %CA. Differences among the populations in activity levels and forms may underlie some of this variation in %CA. The samples in the current study represent two populations of foragers, while the sample used by Macintosh et al. (2013) represented village agriculturalists (#36 Morris Farms of the Oneota cultural tradition). While agricultural subsistence has been found to be associated with reductions in long bone robusticity relative to forager populations, largely due to reduced mobility (Macintosh et al., 2015; Ruff et al., 1984; Sparacello et al., 2011; Sparacello & Marchi, 2008), this is not universally the case and often varies by sex (Macintosh et al., 2017; Ruff, 1987). Cowgill (2010) examined long bone CSG properties of immature skeletons in a wide range of populations from the Late Pleistocene and Holocene of varying subsistence strategies and while there were differences among the samples, there was not a consistent pattern of differences based on subsistence strategy. There are, of course, other factors that may underlie differences in %CA among populations, such as nutritional or other physiological stress, or genetic factors. An additional source of error may be variable morphology captured at locations towards the epiphyseal ends. For some individuals, bony structures such as the developing deltoid tuberosity of the humerus and the lesser trochanter of the femur may be included at the 80% location,

which Macintosh et al. (2013) suggest may result in variation in the true location of the centroid, resulting in larger differences between true and solid CSG estimations. This problem may be exaggerated in immature skeletal material.

While previous studies have found acceptable error rates in adult skeletal samples, in immature individuals, where bone growth is still in progress, varying rates of bone deposition and resorption on the periosteal and endosteal surfaces may result in larger differences between solid and true CSG values. In adults, significant subperiosteal bone cannot be added so only endosteal resorption is affected (Eriksen, 1976; Frisancho et al., 1970; Garn, 1970; Garn et al., 1967; Garn et al., 1969; Lazenby, 1990; Pearson & Lieberman, 2004; Ruff et al., 1994). However, at different points of the growth and development period, bone adaptive responses vary. Late adolescents and young adults, those near or just following the adolescent growth spurt, respond to loading by depositing bone on both the endosteal and periosteal surfaces, while prior to the growth spurt, children increase subperiosteal bone deposition but reduce the rate of endosteal bone resorption rather than adding bone to this surface (Bass et al., 2002; Pearson & Lieberman, 2004; Ruff et al., 1994). Given this, we may have expected %DIF, %PE, and Bias %PE to be correlated with age, but this appears not to be the case. In addition, the limited effect of estimated age on the regression models, once variation accounted for by %CA is controlled for, suggests that age alone does not play a consistent role in generating error. These results indicate that magnitude of error is not constant across the growth and development period perhaps due to variation in bone growth rate and timing, and/or in bone adaptive responses independent of age. Ultimately, there are numerous sources of inter-individual variation in %CA among individuals, and even more so for immature individuals, which results in variation in rate of periosteal deposition and endosteal resorption. These include sex-related differences in the timing and rate of age-related changes to these processes, and when one is working with archeological samples, age at death is estimated, and sex is generally unknown.

This study has shown that when measuring CSG parameters in an ontogenetic sample, it is necessary to include the location of the endosteal contour. Methods of CSG measurement that utilize only the periosteal contour are not recommended, except perhaps if interest is only in diaphyseal shape ( $I_{\max}/I_{\min}$ ). Given that previous studies have shown solid CSG measurements to be within acceptable error limits for adult samples (Davies et al., 2012; MacIntosh et al., 2014; Stock & Shaw, 2007), there is likely a point during later ontogeny where error in periosteal-only CSG parameters is sufficiently reduced for use in biomechanical analyses. Future research with larger samples of adolescents should focus on identifying when that occurs.

#### AUTHOR CONTRIBUTIONS

**Helen K. Kurki:** Conceptualization (equal); data curation (equal); formal analysis (equal); funding acquisition (equal); methodology (equal); project administration (equal); writing – original draft (equal); writing – review and editing (equal). **Sydney Holland:** Formal analysis (equal); writing – original draft (equal); writing – review and editing (equal).

**Marla MacKinnon:** Formal analysis (equal); writing – original draft (equal); writing – review and editing (equal). **Libby W. Cowgill:** Conceptualization (equal); methodology (equal); resources (equal); writing – review and editing (equal). **Benjamin Osipov:** Conceptualization (equal); formal analysis (equal); methodology (equal); writing – review and editing (equal). **Lesley Harrington:** Conceptualization (equal); data curation (equal); formal analysis (equal); funding acquisition (equal); methodology (equal); project administration (equal); writing – review and editing (equal).

## ACKNOWLEDGMENTS

The authors thank the curators and communities who granted access to their collections for this research: Celeste Booth, Albany Museum; Wendy Black and Wilhelmina Seconna, Iziko Museums of South Africa, Cape Town; David Morris, McGregor Museum; the late James Brink, National Museum, Bloemfontein; The Inuit Heritage Trust; Janet Young, Canadian Museum of History. This research was funded by the Natural Sciences and Engineering Research Council of Canada (grant number RGPGP-2014-00054).

## ETHICS STATEMENT

Permission to study the human remains for this research were sought following the procedures established at each curatorial institution. For the Sadlermiut Skeletal Collection, housed at the Canadian Museum of History, this involved consultation with the Inuit Heritage Trust and the Museum curator. The procedures at the remaining institutions involved permissions provided by institutional curators.

## CONFLICT OF INTEREST

The authors declare no conflicts of interest.

## DATA AVAILABILITY STATEMENT

This study involves data from human skeletal remains. Use of these data are limited by permissions provided by curatorial institutions. The data have been freely shared with these institutions and the Inuit Heritage Trust. Researchers may request access to the data by contacting the corresponding author, so that permission for additional research may be sought from the appropriate source.

## ORCID

Helen K. Kurki  <https://orcid.org/0000-0001-9789-6584>

Libby Cowgill  <https://orcid.org/0000-0003-4880-3809>

Benjamin Osipov  <https://orcid.org/0000-0001-9456-3311>

Lesley Harrington  <https://orcid.org/0000-0001-6763-4057>

## REFERENCES

- AlQahtani, S. J., Hector, M. P., & Liversidge, H. M. (2010). Brief communication: The London atlas of human tooth development and eruption. *American Journal of Physical Anthropology*, 142(3), 481–490. <https://doi.org/10.1002/ajpa.21258>
- Bass, S. L., Saxon, L., Daly, R. M., Turner, C. H., Robling, A. G., Seeman, E., & Stuckey, S. (2002). The effect of mechanical loading on the size and shape of bone in pre-, peri-, and postpubertal girls: A study in tennis players. *Journal of Bone and Mineral Research*, 17(12), 2274–2280. <https://doi.org/10.1359/jbmr.2002.17.12.2274>
- Baxter, J. (2005). *The archaeology of childhood: Children, gender and material culture*. Altamira Press.
- Cameron, M. E., & Pfeiffer, S. (2014). Long bone cross-sectional geometric properties of later stone age foragers and herder-foragers. *South African Journal of Science*, 110(9–10), 78–88. <https://doi.org/10.1590/sajs.2014/20130369>
- Cardoso, H. F. V., Abrantes, J., & Humphrey, L. T. (2014). Age estimation of immature human skeletal remains from the diaphyseal length of the long bones in the postnatal period. *International Journal of Legal Medicine*, 128(5), 809–824. <https://doi.org/10.1007/s00414-013-0925-5>
- Cardoso, H. F. V., Spake, L., & Humphrey, L. T. (2017). Age estimation of immature human skeletal remains from the dimensions of the girdle bones in the postnatal period. *American Journal of Physical Anthropology*, 163(4), 772–783. <https://doi.org/10.1002/ajpa.23248>
- Coltrain, J. B., Hayes, M. G., & O'Rourke, D. H. (2004). Sealing, whaling and caribou: The skeletal isotope chemistry of eastern Arctic foragers. *Journal of Archaeological Science*, 31(1), 39–57. <https://doi.org/10.1016/j.jas.2003.06.003>
- Cowgill, L. W. (2010). The ontogeny of Holocene and late Pleistocene human postcranial strength. *American Journal of Physical Anthropology*, 141(1), 16–37. <https://doi.org/10.1002/ajpa.21107>
- Cowgill, L. W. (2014). Femoral diaphyseal shape and mobility: An ontogenetic perspective. In K. J. Carlson & D. Marchi (Eds.), *Reconstructing mobility: Environmental, behavioral, and morphological determinants* (pp. 193–208). Springer. [https://doi.org/10.1007/978-1-4899-7460-0\\_11](https://doi.org/10.1007/978-1-4899-7460-0_11)
- Davies, T., Shaw, C. N., & Stock, J. T. (2012). A test of a new method and software for the rapid estimation of cross-sectional geometric properties of long bone diaphyses from 3D laser surface scans. *Archaeological and Anthropological Sciences*, 4(4), 277–290. <https://doi.org/10.1007/s12520-012-0101-8>
- Davies, T. G., & Stock, J. T. (2014). Human variation in the periosteal geometry of the lower limb: Signatures of behaviour among human Holocene populations. In K. Carlson & D. Marchi (Eds.), *Reconstruction mobility: Environmental, behavioral, and morphological determinants* (pp. 67–90). Springer. <https://doi.org/10.1007/978-1-4899-7460-0>
- Doube, M., Klosowski, M. M., Arganda-Carreras, I., Cordelières, F. P., Dougherty, R. P., Jackson, J. S., Schmid, B., Hutchinson, J. R., & Shefelbine, S. J. (2010). BoneJ: Free and extensible bone image analysis in ImageJ. *Bone*, 47, 1076–1079. <https://doi.org/10.1016/j.bone.2010.08.023>
- Eleazer, C. D., & Jankauskas, R. (2016). Mechanical and metabolic interactions in cortical bone development. *American Journal of Physical Anthropology*, 160(2), 317–333. <https://doi.org/10.1002/ajpa.22967>
- Ericksen, M. F. (1976). Cortical bone loss with age in three native American populations. *American Journal of Physical Anthropology*, 45, 443–452. <https://doi.org/10.1002/ajpa.1330450306>
- Frisancho, A. R., Garn, S. M., & Ascoli, W. (1970). Subperiosteal and endosteal bone apposition during adolescence. *Human Biology*, 42(4), 639–664.
- Garn, S. M. (1970). *The earlier gain and later loss of cortical bone*. Charles C. Thomas.
- Garn, S. M., Guzmán, M. A., & Wagner, B. (1969). Subperiosteal gain and endosteal loss in protein-calorie malnutrition. *American Journal of Physical Anthropology*, 30(1), 153–155. <https://doi.org/10.1002/ajpa.1330300120>
- Garn, S. M., Rohmann, C. G., Wagner, B., & Ascoli, W. (1967). Continuing bone growth throughout life: A general phenomenon. *American Journal of Physical Anthropology*, 26(3), 313–317. <https://doi.org/10.1002/ajpa.1330260306>
- Gooderham, E., Matias, A., Liberato, M., Santos, H., Walshaw, S., Albanese, J., & Cardoso, H. F. V. (2019). Linear and appositional growth in children as indicators of social and economic change during medieval Islamic to Christian transition in Santarém, Portugal. *International Journal of Osteoarchaeology*, 29(5), 736–746. <https://doi.org/10.1002/oa.2784>



- Harrington, L., & Osipov, B. (2018). The developing forager: Reconstructing childhood activity patterns from long bone cross-sectional geometry. In S. Crawford, D. M. Hadley & G. Sheperd (Eds.), *The Oxford Handbook of the Archaeology of Childhood* (pp. 429–446). Oxford Academic. <https://doi.org/10.1093/oxfordhb/9780199670697.013.23>
- Jepsen, K. J. (2009). Systems analysis of bone. *WIREs Systems Biology and Medicine*, 1(1), 73–88. <https://doi.org/10.1002/wsbm.15>
- Lanyon, L. E., Goodship, A. E., Pye, C., & MacFie, J. (1982). Mechanically adaptive bone remodelling. *Journal of Biomechanics*, 15(3), 141–154. [https://doi.org/10.1016/0021-9290\(82\)90246-9](https://doi.org/10.1016/0021-9290(82)90246-9)
- Lanyon, L. E., & Rubin, C. (1984). Static vs. dynamic loads as an influence on bone remodelling. *Journal of Biomechanics*, 17(12), 897–905. [https://doi.org/10.1016/0021-9290\(84\)90003-4](https://doi.org/10.1016/0021-9290(84)90003-4)
- Lazenby, R. A. (1990). Continuing periosteal apposition II: The significance of peak bone mass, strain equilibrium and age-related activity differentials for mechanical compensation in human tubular bones. *American Journal of Physical Anthropology*, 82(4), 473–484. <https://doi.org/10.1002/ajpa.1330820408>
- Lewis, M. (2016). Work and the adolescent in medieval England ad 900–1550: The osteological evidence. *Medieval Archaeology*, 60(1), 138–171. <https://doi.org/10.1080/00766097.2016.1147787>
- Macintosh, A. A., Davies, T. G., Pinhasi, R., & Stock, J. T. (2015). Declining tibial curvature parallels ~6150 years of decreasing mobility in central European agriculturalists. *American Journal of Physical Anthropology*, 157(2), 260–275. <https://doi.org/10.1002/ajpa.22710>
- Macintosh, A. A., Davies, T. G., Ryan, T. M., Shaw, C. N., & Stock, J. T. (2013). Periosteal versus true cross-sectional geometry: A comparison along humeral, femoral, and tibial diaphyses. *American Journal of Physical Anthropology*, 150(3), 442–452. <https://doi.org/10.1002/ajpa.22218>
- Macintosh, A. A., Pinhasi, R., & Stock, J. T. (2017). Prehistoric women's manual labor exceeded that of athletes through the first 5500 years of farming in Central Europe. *Science Advances*, 3(11), ea03893. <https://doi.org/10.1126/sciadv.aao3893>
- Mays, S., Ives, R., & Brickley, M. (2009). The effects of socioeconomic status on endochondral and appositional bone growth, and acquisition of cortical bone in children from 19th century Birmingham, England. *American Journal of Physical Anthropology*, 140(3), 410–416. <https://doi.org/10.1002/ajpa.21076>
- Merbs, C. F. (1983). *Patterns of activity-induced pathology in a Canadian Inuit population*. Number 119 in National Museum of Man Archaeological Survey of Canada Mercury Series. National Museum of Man.
- Miller, M. J., Agarwal, S. C., Aristizabal, L., & Langebaek, C. (2018). The daily grind: Sex- and age-related activity patterns inferred from cross-sectional geometry of long bones in a pre-Columbian muisca population from Tibanica, Colombia. *American Journal of Physical Anthropology*, 167(2), 311–326. <https://doi.org/10.1002/ajpa.23629>
- Mizushima, S., Suwa, G., & Hirata, K. (2016). A comparative analysis of fetal to subadult femoral midshaft bone distribution of prehistoric Jomon hunter-gatherers and modern Japanese. *Anthropological Science*, 124(1), 1–15. <https://doi.org/10.1537/ase.151104>
- Morris, A. (1992). *The skeletons of contact: A study of protohistoric burials from the lower Orange River valley, South Africa*. Witwatersrand University Press.
- Nowell, A. (2021). *Growing up in the ice age: Fossil and archaeological evidence of the lived lives of Plio-Pleistocene children*. Oxbow Books.
- O'Neill, M. C., & Ruff, C. B. (2004). Estimating human long bone cross-sectional geometric properties: A comparison of noninvasive methods. *Journal of Human Evolution*, 47(4), 221–235. <https://doi.org/10.1016/j.jhevol.2004.07.002>
- Osipov, B., Harrington, L., Temple, D., Bazaliiskii, V. I., & Weber, A. W. (2020). Chronological and regional variation in developmental stress and behavior of early and late Neolithic cis-Baikal hunter-gatherer juveniles: Insights from diaphyseal cross-sectional geometry. *Archaeological Research in Asia*, 24, 100231. <https://doi.org/10.1016/j.ara.2020.100231>
- Osipov, B., Temple, D., Cowgill, L., Harrington, L., Bazaliiskii, V. I., & Weber, A. W. (2016). Evidence for genetic and behavioral adaptations in the ontogeny of prehistoric hunter-gatherer limb robusticity. *Quaternary International*, 405(B), 134–146. <https://doi.org/10.1016/j.quaint.2015.09.093>
- Pearson, O. M., & Lieberman, D. E. (2004). The aging of Wolff's "law": Ontogeny and responses to mechanical loading in cortical bone. *American Journal of Physical Anthropology*, 125(S39), 63–99. <https://doi.org/10.1002/ajpa.20155>
- Pearson, O. M., Petersen, T. R., Sparacello, V. S., Daneshvari, S. R., & Grine, F. E. (2014). Activity, "body shape," and cross-sectional geometry of the femur and tibia. In K. J. Carlson & D. Marchi (Eds.), *Reconstructing mobility: Environmental, behavioral, and morphological determinants* (pp. 133–151). Springer. [https://doi.org/10.1007/978-1-4899-7460-0\\_8](https://doi.org/10.1007/978-1-4899-7460-0_8)
- Pfeiffer, S., & Harrington, L. (2011). Bioarchaeological evidence for the basis of small adult stature in southern Africa: Growth, mortality, and small stature. *Current Anthropology*, 52, 449–461. <https://doi.org/10.1086/659452>
- R Core Team. (2019). R: A language and environment for statistical computing (version 3.6.1) [Software]. <https://www.R-project.org/>.
- Ruff, C. B. (1987). Sexual dimorphism in human lower limb bone structure: Relationship to subsistence strategy and sexual division of labor. *Journal of Human Evolution*, 16, 391–416. [https://doi.org/10.1016/0047-2484\(87\)90069-8](https://doi.org/10.1016/0047-2484(87)90069-8)
- Ruff, C. B. (1994). Biomechanical analysis of northern and southern plains femora: Behavioral implications. In D. W. Owsley & R. L. Jantz (Eds.), *Skeletal biology in the Great Plains: Migration, warfare, health, and subsistence* (pp. 235–245). Smithsonian Institution Press.
- Ruff, C. B. (2002). Long bone articular and diaphyseal structure in Old World monkeys and apes, I: Locomotor effects. *American Journal of Physical Anthropology*, 119, 305–342.
- Ruff, C. B. (2003a). Growth in bone strength, body size, and muscle size in a juvenile longitudinal sample. *Bone*, 33(3), 317–329. [https://doi.org/10.1016/s8756-3282\(03\)00161-3](https://doi.org/10.1016/s8756-3282(03)00161-3)
- Ruff, C. B. (2003b). Ontogenetic adaptation to bipedalism: Age changes in femoral to humeral length and strength proportions in humans, with a comparison to baboons. *Journal of Human Evolution*, 45(4), 317–349. <https://doi.org/10.1016/j.jhevol.2003.08.006>
- Ruff, C. B. (2003c). Long bone articular and diaphyseal structures in Old World monkeys and apes. II: Estimation of body mass. *American Journal of Physical Anthropology*, 120(1), 16–37. <https://doi.org/10.1002/ajpa.10118>
- Ruff, C. B. (2019). Biomechanical analyses of archaeological human skeletons. In M. A. Katzenberg & A. L. Grauer (Eds.), *Biological anthropology of the human skeleton* (Third ed., pp. 189–224). John Wiley & Sons, Inc.. <https://doi.org/10.1002/9781119151647.ch6>
- Ruff, C. B., & Hayes, W. (1983). Cross-sectional geometry of Pecos Pueblo femora and tibiae—A biomechanical investigation: I. method and general patterns of variation. *American Journal of Physical Anthropology*, 60(3), 359–381. <https://doi.org/10.1002/ajpa.1330600308>
- Ruff, C. B., Holt, B., Niskanen, M., Sladek, V., Berner, M., Garofalo, E., Garvin, H. M., Hora, M., Junno, J. A., Schuplerova, E., Vilkkama, R., & Whittey, E. (2015). Gradual decline in mobility with the adoption of food production in Europe. *Proceedings of the National Academy of Sciences of the United States of America*, 112(23), 7147–7152. <https://doi.org/10.1073/pnas.1502932112>
- Ruff, C. B., Holt, B., & Trinkaus, E. (2006). Who's afraid of the big bad Wolff?: "Wolff's law" and bone functional adaptation. *American Journal of Physical Anthropology*, 129(4), 484–498. <https://doi.org/10.1002/ajpa.20371>
- Ruff, C. B., & Larsen, C. S. (2014). Long bone structural analyses and the reconstruction of past mobility: A historical review. In K. J. Carlson & D. Marchi (Eds.), *Reconstructing mobility: Environmental, behavioral, and*



- morphological determinants (pp. 13–29). Springer US. [https://doi.org/10.1007/978-1-4899-7460-0\\_2](https://doi.org/10.1007/978-1-4899-7460-0_2)
- Ruff, C. B., Larsen, C. S., & Hayes, W. (1984). Structural changes in the femur with the transition to agriculture on the Georgia coast. *American Journal of Physical Anthropology*, 64(2), 125–136. <https://doi.org/10.1002/ajpa.1330640205>
- Ruff, C. B., Walker, A., & Trinkaus, E. (1994). Postcranial robusticity in homo. III: Ontogeny. *American Journal of Physical Anthropology*, 9(1), 35–54. <https://doi.org/10.1002/ajpa.1330930103>
- Schindelin, J., Arganda-Carreras, I., Frise, E., Kaynig, V., Longair, M., Pietzsch, T., Rueden, C., Saalfeld, S., Schmid, B., Tinevez, J. Y., White, D. J., Hartenstein, V., Eliceiri, K., Tomancak, P., & Cardona, A. (2012). Fiji: An open-source platform for biological-image analysis. *Nature Methods*, 9(7), 676–682. <https://doi.org/10.1038/nmeth.2019>
- Shaw, C. N., & Stock, J. T. (2013). Extreme mobility in the late Pleistocene? Comparing limb biomechanics among fossil homo, varsity athletes and Holocene foragers. *Journal of Human Evolution*, 64(4), 242–249. <https://doi.org/10.1016/j.jhevol.2013.01.004>
- Shaw, C. N., Stock, J. T., Davies, T. G., & Ryan, T. M. (2014). Does the distribution and variation in cortical bone along lower limb diaphyses reflect selection for locomotor economy? In K. Carlson & D. Marchi (Eds.), *Mobility: Interpreting behavior from skeletal adaptations and environmental interactions* (pp. 49–66). Springer. [https://doi.org/10.1007/978-1-4899-7460-0\\_4](https://doi.org/10.1007/978-1-4899-7460-0_4)
- Sparacello, V., & Marchi, D. (2008). Mobility and subsistence economy: A diachronic comparison between two groups settled in the same geographical area (Liguria, Italy). *American Journal of Physical Anthropology*, 136(4), 485–495. <https://doi.org/10.1002/ajpa.20832>
- Sparacello, V. S., & Pearson, O. M. (2010). The importance of accounting for the area of the medullary cavity in cross-sectional geometry: A test based on the femoral midshaft. *American Journal of Physical Anthropology*, 143(4), 612–624. <https://doi.org/10.1002/ajpa.21361>
- Sparacello, V. S., Pearson, O. M., Coppa, A., & Marchi, D. (2011). Changes in skeletal robusticity in an iron age agropastoral group: The Samnites from the Alfedena necropolis (Abruzzo, Central Italy). *American Journal of Physical Anthropology*, 144(1), 119–130. <https://doi.org/10.1002/ajpa.21377>
- Stock, J., & Pfeiffer, S. (2001). Linking structural variability in long bone diaphyses to habitual behaviors: Foragers from the southern African later stone age and the Andaman Islands. *American Journal of Physical Anthropology*, 115(4), 337–348. <https://doi.org/10.1002/ajpa.1090>
- Stock, J., & Pfeiffer, S. (2004). Long bone robusticity and subsistence behaviour among later stone age foragers of the forest and fynbos biomes of South Africa. *Journal of Archaeological Science*, 31(7), 999–1013. <https://doi.org/10.1016/j.jas.2003.12.012>
- Stock, J. T. (2002). A test of two methods of radiographically deriving long bone cross-sectional properties compared to direct sectioning of the diaphysis. *International Journal of Osteoarchaeology*, 12(5), 335–342. <https://doi.org/10.1002/oa.629>
- Stock, J. T., & Shaw, C. N. (2007). Which measures of diaphyseal robusticity are robust? A comparison of external methods of quantifying the strength of long bone diaphyses to cross-sectional geometric properties. *American Journal of Physical Anthropology*, 134(3), 412–423. <https://doi.org/10.1002/ajpa.20686>
- Stock, J. T., Shirley, M. K., Sarringhaus, L. A., Davies, T. G., & Shaw, C. N. (2013). Skeletal evidence for variable patterns of handedness in chimpanzees, human hunter-gatherers, and recent British populations. *Annals of the New York Academy of Sciences*, 1288(1), 86–99. <https://doi.org/10.1111/nyas.12067>
- Sylvester, A. D., Garofalo, E., & Ruff, C. (2010). Technical note: An R program for automating bone cross section reconstruction. *American Journal of Physical Anthropology*, 142(4), 665–669. <https://doi.org/10.1002/ajpa.21299>
- Temple, D. H., Bazaliiskii, V. I., Goriunova, O. I., & Weber, A. W. (2014). Skeletal growth in early and late Neolithic foragers from the cis-Baikal region of eastern Siberia. *American Journal of Physical Anthropology*, 153(3), 377–386. <https://doi.org/10.1002/ajpa.22436>
- Trinkaus, E., & Ruff, C. B. (1989). Diaphyseal cross-sectional morphology and biomechanics of the fond-de-Forêt 1 femur and the spy 2 femur and tibia. *Anthropologie et Préhistoire*, 100, 33–42.

## SUPPORTING INFORMATION

Additional supporting information can be found online in the Supporting Information section at the end of this article.

**How to cite this article:** Kurki, H. K., Holland, S., MacKinnon, M., Cowgill, L., Osipov, B., & Harrington, L. (2022). Appositional long bone growth: Implications for measuring cross-sectional geometry. *American Journal of Biological Anthropology*, 1–16. <https://doi.org/10.1002/ajpa.24602>